

CHARACTERIZATION AND THERMOELECTRIC PROPERTIES OF Na-Co-O THIN FILMS BY PULSED-DC MAGNETRON SPUTTERING

Weerasak Somkhunthot^{a*}, Thanusit Burinprakhon^b and Nuwat Pimpabute^a

^a Program of Physics, Faculty of Science and Technology, Loei Rajabhat University
234 Loei-Chiangkan Road, Amphoe Muang, Loei, 42000, Thailand

^b Physics Department, Faculty of Science, Khon Kaen University 123 Mittaparp Road, Muang District,
Khon Kaen 40002, Thailand

Received 15 July 2012; accepted 30 August 2012

ABSTRACT

The built bipolar pulsed-dc magnetron sputtering was used to synthesize Na-Co-O thin films on glass substrates from a $\text{Na}_x\text{Co}_2\text{O}_4$ ($x > 1.5$) target under argon atmosphere. The sputtering target was a pellet of 60 mm diameter, 2.5 mm thick, and 3.17 g/cm^3 density which was made by the sintering of $\text{Na}_x\text{Co}_2\text{O}_4$ ($x > 1.5$) powder precursors obtained from a polymerized complex (PC) method. The depositions were carried out at the argon gas flow rates of 16.7 and 23.3 sccm, the pulsed frequency of 17 kHz, and the reverse positive pulse of 100 V. The sputtering powers of 38 W (380 V 100 mA) and 45 W (390 V 120 mA) were used for depositing the films. The optical emissions from the plasma during the deposition were measured in the wavelength range of 360-800 nm using a high resolution spectrometer. The deposited films were then subjected to annealing at 733 K in air for 3 h. The crystal structure of as deposited films and annealed films were studied by XRD. The film thickness was obtained from the Ellipsometric measurement. The thermoelectric properties of the films were assessed by Seebeck coefficient and electrical resistivity measurements at room temperature. The Seebeck coefficient of the films was obtained from the measurement of Seebeck emf as a function of temperature difference across the film surface. The electrical resistivity was measured by the standard Van der Pauw four-probe method. It was found that pulsed-dc magnetron plasmas were successfully generated to enable the deposition of the Na-Co-O containing thin films from the $\text{Na}_x\text{Co}_2\text{O}_4$ ($x > 1.5$) target onto the glass substrates. XRD results showed that the as-deposited films were amorphous. Results from optical emission analysis, XRD analysis, and thermoelectric properties measurement indicated that the films annealed at 773 K for 3 h were polycrystalline $\text{Na}_x\text{Co}_2\text{O}_4$ having (100) preferred orientation, with Co_3O_4 as a secondary phase. Hot probe test indicated that all film samples exhibited p-type conduction. The as-deposited and annealed films showed the larger thermoelectric power, higher electrical resistivity, and, hence, lower power factor than the pellet used as the sputtering target. In addition, the thermoelectric power increased with increasing the discharge power and decreasing gas flow rate. The annealing process at 773 K, in air, improved the power factor by one order magnitude. These preliminary studies demonstrated that repeatability of the deposition process and thin film properties can be achieved from the built system. Therefore, it can be used as an important platform for further thin film research.

KEYWORDS: pulsed-dc magnetron sputtering, thermoelectric properties, Na-Co-O thin films

*

Corresponding authors; e-mail: weerasak1963@yahoo.co.th, Tel.: +66-4283-5238, Fax: +66-4283-5238

INTRODUCTION

The performance of a thermoelectric device is determined by the dimensionless figure of merit

ZT given by $ZT = S^2T/\rho\kappa$. The thermoelectric parameters S , ρ , κ are the Seebeck coefficient, the electrical resistivity, and the thermal conductivity of the thermoelectric materials used to fabricate

the device, respectively. T is the absolute temperature in K at which the device operates. Higher ZT values lead to thermoelectric devices of improved performance. In other words, good thermoelectric materials, which are defined as materials of high S , low ρ , and low κ , are crucial for the fabrication of high efficiency thermoelectric devices. The thermoelectric parameters S , κ , ρ , and, hence, ZT are dependent on materials and their properties. The highest ZT of about 1.0 has been achieved from the state of the art thermoelectric material Bi_2Te_3 and Sb_2Te_3 at room temperature [1, 2]. Both theoretical and experimental approaches have been conducted to search for new materials of higher ZT . This has been the important task in the development of thermoelectric technology.

Among those materials investigated, a transition metal oxide $\text{Na}_x\text{Co}_2\text{O}_4$ has been expected to be one of the candidates for good thermoelectric materials. This new thermoelectric material has been reported to exhibit a large thermoelectric power with a low resistivity [3]. Its room temperature ZT value is comparable to that of Bi_2Te_3 [4]. This finding has triggered intensive studies on the thermoelectric properties of the material. Within the past few years, there have been a number of papers reporting the preparation of powder and bulk $\text{Na}_x\text{Co}_2\text{O}_4$ by several methods including the conventional solid state reaction (SSR) method and the polymerized complex (PC) method or citric acid complex (CAC) method. It has been found that the thermoelectric properties of $\text{Na}_x\text{Co}_2\text{O}_4$ are dependent on the preparation method and types of metal added [5]. The Seebeck coefficient of PC or CAC samples is significantly higher than that of SSR samples. The maximum ZT value of 0.8 was obtained for the PC sample at 955 K, which is higher than ZT value of 0.5 for the SSR sample [6, 7]. The improvement in ZT is believed to be due to the finer crystalline grain sizes of the sample prepared through the PC route. Doping with metals such as Ag shows strong influence on the thermoelectric properties of $\text{Na}_x\text{Co}_2\text{O}_4$ [8, 9]. For example, the ZT of an Ag-doped sample was found to be higher than that of the non-doped sample, and reached ZT of 0.12 at 973 K while the non-doped sample reached ZT of 0.11 at 973 K [10, 11].

Although there have been a number of studies on the fabrication and thermoelectric properties of $\text{Na}_x\text{Co}_2\text{O}_4$, most of the previous work has concentrated on the bulk form of this material and, as such, not much attention has been paid to

thin films of $\text{Na}_x\text{Co}_2\text{O}_4$. In general, thermoelectric materials fabricated in the form of thin films are of interest for applications where small scale thermoelectric heating/cooling or powering is required. In addition, thin films of several thermoelectric materials have been shown to exhibit improved thermoelectric properties, as compared to those of the bulk form. A maximum ZT of 2.4 at room temperature was observed in the $\text{Bi}_2\text{Te}_3/\text{Sb}_2\text{Te}_3$ superlattice devices [12]. The power factor of $\text{B}_{12+x}\text{C}_{3-x}$ thin films was higher than that of the bulk specimen [13]. The electrical resistivity of thin films was relatively low compared with that of a bulk specimen for Zn_4Sb_3 compounds [14]. Bi_2Te_3 thin films were shown to have a linear function between electrical resistivity and the reciprocal of film thickness [15]. Besides, the CuAlO_2 thin films showed considerably high values of thermoelectric power and enhanced dimensionless figure of merit [16]. The $\text{Nd}_{0.75}\text{-Sr}_{1.25}\text{CoO}_4$ thin film was discovered to have a large power factor [17].

Thin films of $\gamma\text{-Na}_x\text{CoO}_2$ have been successfully deposited using the pulsed laser deposition (PLD). Recently, epitaxial $\gamma\text{-Na}_x\text{CoO}_2$ thin films were deposited on (001) sapphire by the PLD. It is inferred that the structural strain is the source for the lower resistivity and the preservation of the strongly correlated system up to 200 K for the $\text{Na}_{0.7}\text{CoO}_2$ thin film [18]. The resistivity and Seebeck coefficient showed linear increase with temperature [19]. The films were stable in vacuum or in a pure oxygen environment, but were not stable in air, causing their resistivity to increase exponentially with time until they became semiconductors or insulators [20]. Films grown at high temperatures of 500°C and 600°C showed lower resistivity and the largest thermopower in the range of 10.7 mΩ·cm - 721 μΩ·cm and 35 - 100 μV/K at room temperature, respectively [21]. It is a goal here to conduct further investigation on the properties of the Na_xCoO_2 thin films prepared by the well known magnetron sputtering technology. This could widen the potential for applications of this material.

Magnetron sputtering is one of the physical vapor deposition (PVD) methods which are widely used in thin film technology. The various types of magnetron sputtering technique are alternating current (ac), radio frequency (rf), direct current (dc), and pulsed-dc. A pulsed-dc magnetron sputtering technique is one of the latest developments in sputtering technology and has many advantages over others, since it is

versatile and provides an ability to deposit thin films of oxide compounds such as Al_2O_3 , ITO, and ZnO at high deposition rate and to eliminate arcing problems of poisoned targets [22]. Since the year 2000-2006, this technique has been a well developed deposition method for coatings and thin films used in research and in industrial applications [23-32]. It is of interest to apply this deposition technology to the preparation of $\text{Na}_x\text{Co}_2\text{O}_4$ thin films. It may be possible to customize the deposition conditions so that a $\text{Na}_x\text{Co}_2\text{O}_4$ thin film of highly preferred orientation can be grown. Such a film could give interesting thermoelectric properties due to its electrical and thermal anisotropy [4].

In the present paper, the deposition of thin films synthesized by pulsed-dc magnetron sputtering of a $\text{Na}_x\text{Co}_2\text{O}_4$ target in an argon atmosphere under varying Ar flow rate and sputtering power. The properties of the $\text{Na}_x\text{Co}_2\text{O}_4$ thin films including crystalline structure and thermoelectric properties will be investigated as a function of deposition conditions. The effects of discharge power and the sputtering gas flow rate (Ar) on the film properties will be focused. This study will give an insight into the relationship between the thermoelectric properties of the $\text{Na}_x\text{Co}_2\text{O}_4$ thin films and deposition conditions, and may shed light on the potential applications of this material.

MATERIALS AND METHODS

The experimental details of the deposition conditions, post-deposition annealing, plasma and thin film characterization, and thermoelectric properties measurement are given below.

1. Deposition Conditions

The depositions of $\text{Na}_x\text{Co}_2\text{O}_4$ thin films have been carried out using an in-house-built pulsed-dc magnetron sputtering system. The details of design and construction of the system has been reported elsewhere [33-34]. The sputtering target was a $\text{Na}_x\text{Co}_2\text{O}_4$ ($x > 1.5$) pellet of 60 mm diameter, 2.5 mm thick, and 3.17 g/cm^3 density. The target was made by sintering powder precursors obtained from a polymerized complex (PC) route [35].

In this experiment, the glass slides of $1.5 \times 1.5 \text{ cm}^2$ were used as substrate. The substrates were placed at a distance of 5.0 cm above the target and no additional heating was applied. To

generate the pulsed-dc plasma and initiate the thin film deposition, the vacuum chamber was pumped down to a base pressure of 15 mtorr and flushed with high purity argon (Ar 99.999%) for several cycles to ensure the cleanliness of the chamber. In order to survey the possible condition for growing $\text{Na}_x\text{Co}_2\text{O}_4$ films. Two sets of condition were used, as shown in Table 1. From this table, the samples A1, A2, A3, and B1, B2, B3 were deposited by varying Ar flow rate with two different values of 23.3 ± 0.1 and 16.7 ± 0.1 sccm, respectively, while the pulsed frequency is fixed at 17 kHz. The reverse positive pulse was set to be the same current-voltage of 20 mA and 100 V. The sputtering voltage and current of the samples A and B are kept constant of 380 V, 100 mA and 390 V, 120 mA, respectively, corresponding the power of 38 and 45 W. Also in order to test the repeatability of the system conditions were repeated 3 times.

2. Post-Deposition Annealing

Two as-deposited samples from each lot were subjected to post-deposition annealing in air to increase oxygen content in the film and to promote crystal growth. The annealing temperature of 773 K and annealing time of 3 hours were used.

3. Plasma and Thin Film Characterization

The optical emissions from plasma during thin film deposition were observed in the wavelength range of 360-800 nm by the getSpec-2048 spectrometer (Sentronic GmbH). The spectral lines were indexed to the ASD data information of NIST (National Institute of Standards and Technology) [36]. Film thickness was measured using the Ellipsometer (Model L115S300, Gaertner Scientific Corporation, USA). The crystal structure were investigated by X-ray diffractometer equipped with $\text{CuK}\alpha$ radiation, $\lambda = 0.15406 \text{ nm}$. The scanning mode was θ - 2θ with scanning range and rate of $10^\circ \leq 2\theta \leq 70^\circ$ with and $0.02^\circ / \text{sec}$, respectively.

4. Thermoelectric Properties Measurement

Thermoelectric properties were measured at the room temperature in air. Type of charge carrier was determined by hot probe method. Seebeck coefficient (S) was measured using the relation between thermoelectric voltage (ΔV) and the temperature difference (ΔT), $S = \Delta V / \Delta T$. The experimental setup of thermoelectric sensitivity is shown in Fig. 1. The hot and cold junctions

between the across two ends of a film are connected to the digital voltmeter (KEITHLEY 617 PROGRAMMABLE ELECTROMETER). The temperatures T_H and T_C are sensed by the type K thermocouples which are connected to the digital thermometers (7563 DIGITAL THERMOMETER, YOKOGAWA). The resistor of 10 W, 5 Ω was used to heat the hot junction by applying a constant currents to the resistor placed on the hot side. Electrical characteristics were measured by four-point probe method which can be conveniently determined using the Vander Pauw resistivity measurement technique [37]. The electrical resistivity (ρ) of the sample can be estimated by use of the equation, $\rho = (\pi t / \ln 2) [(R_{ab,dc} + R_{bc,ad}) / 2] F [R_{ab,dc} / R_{bc,ad}]$, where t is the thickness of thin film, $R_{ab,dc} = \Delta V_{dc} / I_{ab}$, $R_{bc,ad} = \Delta V_{ad} / I_{bc}$, and F is correction function which can be calculated from $(R_{ab,dc} - R_{bc,ad}) / (R_{ab,dc} + R_{bc,ad}) = (F / \ln 2) \operatorname{arccosh}[\exp(\ln 2 / F) / 2]$. The experimental setup of electrical characteristics is shown in Fig. 2. All contacts were made by silver paste which showed ohmic characteristics over a wide range of currents. The current-voltage characteristic for the measurement of electrical resistivity is measured by using the Keithley instruments. The power factor (P) was calculated from the S and the ρ in the equation, $P = S^2 / \rho$.

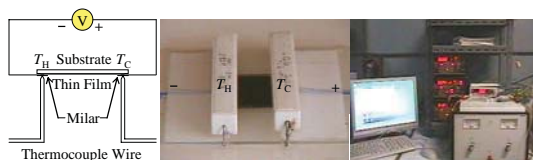


Fig. 1. Experimental setup of thermoelectric sensitivity

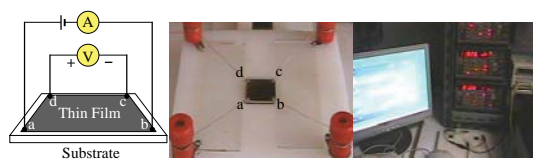


Fig. 2. Experimental setup of electrical characteristics

Table 1. Deposition conditions

Samples	Ar Flow Rate (sccm)	$+t_{off}$ (μ s)	$+t_{on}$ (μ s)	$-t_{off}$ (μ s)	$-t_{on}$ (μ s)	f (kHz)	Sputtering Power		
							I (mA)	V (V)	P (W)
A1, A2, A3	23.3 \pm 0.1	14	10	14	20	17	100	380	38 \pm 1
B1, B2, B3	16.7 \pm 0.1	14	10	14	20	17	120	390	45 \pm 1

RESULTS AND DISCUSSION

To produce Na-Co-O thin films, the $\text{Na}_x\text{Co}_2\text{O}_4$ ($x > 1.5$) pellet obtained in the previous sintering were used as a sputtering target.

1. Plasma Diagnostic

The cathode voltage waveform for $V_{dc1} = 100$ V and $V_{dc2} = -400$ V is shown in Fig. 3(a). Photograph of the stable glow discharge is shown in Fig. 3(b). These results indicate a good pulsed-dc plasma characteristic. The optical emission spectrum of the plasma is shown in Fig. 4. It was found that only the optical emissions of argon were detected at $V_{dc2} = -300$ V, $I_{S2} = 50$ mA, as shown in Fig. 4(a). The optical emissions of sodium (Na) and cobalt (Co) immerges at $V_{dc2} = -300$ V, $I_{S2} = 75$ mA as shown in Fig. 4(b). These lines are clearly seen at higher V_{dc2} as shown in Fig. 4(c, d). In these spectrums, the emission lines of Ar (696.54, 706.72, 738.39, ..., 801.48 nm) and Na (588.99, 589.59 nm) are prominent features. The emission lines of Co and O were detected, but are not intense due to the strong lines of these species are not in the measured range. The optical emission spectrum shows that Na, Co, O atoms were sputtered from the target. Hence, it can be expected that the deposited films will contain these atomic species. From this point onward, the deposited film will be referred to as Na-Co-O containing.

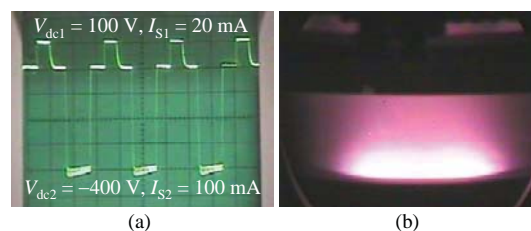


Fig. 3. Waveform and photograph of the pulsed-dc magnetron argon discharge during the sputtering of a $\text{Na}_x\text{Co}_2\text{O}_4$ ($x > 1.5$) target

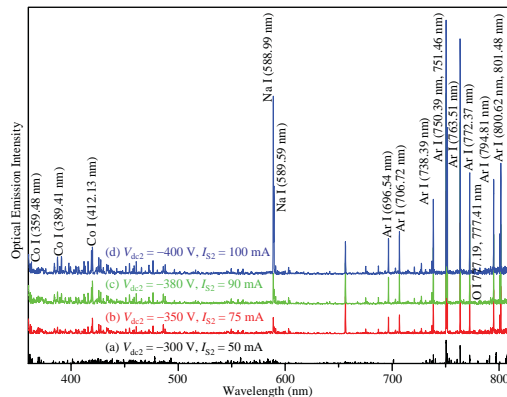


Fig. 4. the optical emission spectrum of the pulsed-dc magnetron argon discharge during the sputtering of a $\text{Na}_x\text{Co}_2\text{O}_4$ ($x > 1.5$) target

2. Crystal Structure

The XRD patterns measured at room temperature of the as-deposited and the annealed films are shown in Figure 5 (samples A1, A2, and A3) and Figure 6 (samples B1, B2, and B3). The XRD patterns in Figure 5(a) and 6(a) clearly show the amorphous nature of the as-deposited films. This was expected since the substrates were not heated during the deposition process. Therefore, the kinetic energy of atomic species at the substrate surface was not enough to promote the growth of a crystal. After annealing process at temperature 773 K, there exists a strong XRD peak centered at $2\theta = 36.8^\circ$. Additional peaks at $2\theta = 31.3^\circ$ and 59.5° are also observed for some annealed samples.

The results indicate the formation of crystalline phases in the annealed films. The strong peaks can be indexed to the diffraction from the (100) plane of NaCo_2O_4 or the (311) plane of Co_3O_4 (JCPDS file number 73-0133 and 78-1970, respectively). The additional peaks observed at $2\theta = 31.3^\circ$ corresponding to (004) plane of $\text{Na}_x\text{Co}_2\text{O}_4$ or the (220) plane of Co_3O_4 phase. Thus, the XRD results show the traces of Co_3O_4 and $\text{Na}_x\text{Co}_2\text{O}_4$ phases in the annealed films. In the latter case, it is interesting that the $\text{Na}_x\text{Co}_2\text{O}_4$ phase exhibits a (100) preferred orientation. This could be of interest for applications in which the anisotropic properties of this material are utilized. It may be summarized at this point that all the as-deposited films are amorphous. This is not surprising due to the fact that the depositions were undertaken at low temperature, at which the energy of the deposited species were not high enough to

promote the crystal formation. After annealing at 773 K for 3 hours, the crystallites of $\text{Na}_x\text{Co}_2\text{O}_4$ and/or Co_3O_4 are grown. The single peak (100) indexed for the $\text{Na}_x\text{Co}_2\text{O}_4$ suggests that the $\text{Na}_x\text{Co}_2\text{O}_4$ crystallites exhibit the (100) preferred orientation. This is rather unusual when compared to the case of bulk pellet in which the (002) preferred orientation occurred as a result of (002) layered structure of the grains [35]. Further investigation is needed to answer this behavior.

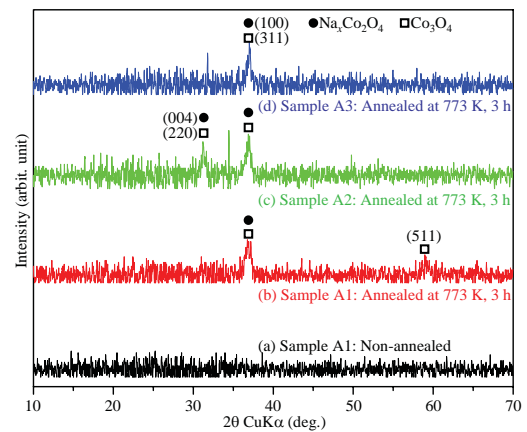


Fig. 5. XRD patterns of the samples A1, A2, and A3 (at pulse frequency of 17 kHz and Ar flow rate of 23.3 ± 0.1 sccm)

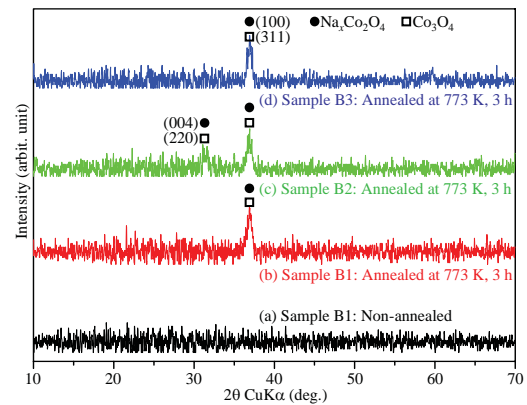


Fig. 6. XRD patterns of the samples B1, B2, and B3 (at pulse frequency of 17 kHz and Ar flow rate of 16.7 ± 0.1 sccm)

3. Thermoelectric Properties of Na-Co-O Thin Films

The type of charge carrier of the deposited films was determined by hot probe method. The cold junction shows higher voltage than the hot junction indicating p-type conduction. All the

non-annealed and annealed films present p-type conduction. The p-type conduction are normally observed for γ -phase $\text{Na}_x\text{Co}_2\text{O}_4$ [7, 11]. The results suggest that the deposited films should contain γ -phase $\text{Na}_x\text{Co}_2\text{O}_4$. An example of the relation between the Seebeck emf and temperature difference is shown in Fig. 7. From this figure, the film exhibits linear dependence between the Seebeck emf of the Na-Co-O film and temperature difference. This result indicates the validity of measurement set up. Fig. 8 shows an example of the current-voltage characteristics obtain from Van der Pauw four-probe measurement. It can be seen that this plot exhibits a good ohmic I - V characteristic. This result shows the validity of experimental set up for Van der Pauw measurement. The results of thickness, Seebeck coefficient (S), and electrical resistivity (ρ) measurements, and the calculated power factor (P) are summarized in Table 2 and 3. The corresponding deposition conditions for the samples examined, Ar flow rate, discharge currents and voltages, are also presented in the tables.

coefficient of 106 $\mu\text{V/K}$ at room temperature. The S of the films are also larger than those reported by Venimadhav et al. for $\text{Na}_x\text{Co}_2\text{O}_4$ film deposited by PLD technique, which gave S in the range of 70-100 $\mu\text{V/K}$ at room temperature [21]. Meanwhile, the resistivities of the non-annealed and annealed samples are in the range of 4.0-5.0 $\Omega\cdot\text{m}$ and 0.3-0.4 $\Omega\cdot\text{m}$, respectively. The resistivity of the Na-Co-O films are very large, as compared to those of the pellet $\text{Na}_x\text{Co}_2\text{O}_4$ samples used as the sputtering target [35] and the value reported by Venimadhav et al. [21], which gave a room temperature value of 0.008 $\Omega\cdot\text{m}$ and 0.0001 $\Omega\cdot\text{m}$, respectively.

The Seebeck coefficient of the annealed Na-Co-O films obtained in this work are found to be about 7 to 13 times as large as the of Co_3O_4 films reported by Kadam and Patil, giving the room temperature values from 7 to 31 $\mu\text{V/K}$ [38]. In addition, The electrical resistivity of the annealed Na-Co-O films are found to be about 1/500 to 1/30 times to that of Co_3O_4 films reported by the same authors giving the room temperature resistivity of 9 to 200 $\Omega\cdot\text{m}$.

Table 2. Thickness, S , ρ , and P of the samples A1, A2, and A3 deposited at pulse frequency of 17 kHz, Ar flow rate of 23.3 ± 0.1 sccm, and sputtering power of 38 W (100 mA, 380 V)

Samples	Thickness (\AA)	S ($\mu\text{V/K}$)	ρ ($\Omega\cdot\text{m}$)	P ($\mu\text{W/m}\cdot\text{K}^2$)
A1: Non-annealed	1248 \pm 38	318 \pm 10	5.0 \pm 0.1	0.02 \pm 0.01
A1: Annealed*	1217 \pm 19	233 \pm 13	0.42 \pm 0.01	0.13 \pm 0.01
A2: Non-annealed	1332 \pm 71	331 \pm 14	5.4 \pm 0.1	0.02 \pm 0.01
A2: Annealed*	1278 \pm 47	265 \pm 12	0.44 \pm 0.01	0.16 \pm 0.01
A3: Non-annealed	1276 \pm 244	322 \pm 10	5.0 \pm 0.3	0.02 \pm 0.01
A3: Annealed*	1261 \pm 111	243 \pm 10	0.44 \pm 0.01	0.13 \pm 0.02

*The annealing temperature of 773 K and annealing time of 3 hours

Table 3. Thickness, S , ρ , and P of the samples B1, B2, and B3 deposited at pulse frequency of 17 kHz, Ar flow rate of 16.7 ± 0.1 sccm, and sputtering power of 45 W (120 mA, 390 V)

Samples	Thickness (\AA)	S ($\mu\text{V/K}$)	ρ ($\Omega\cdot\text{m}$)	P ($\mu\text{W/m}\cdot\text{K}^2$)
B1: Non-annealed	1284 \pm 181	420 \pm 20	4.0 \pm 0.1	0.04 \pm 0.01
B1: Annealed*	1214 \pm 74	300 \pm 6	0.29 \pm 0.01	0.31 \pm 0.02
B2: Non-annealed	1294 \pm 340	417 \pm 24	3.9 \pm 0.2	0.04 \pm 0.01
B2: Annealed*	1251 \pm 35	282 \pm 7	0.30 \pm 0.01	0.27 \pm 0.02
B3: Non-annealed	1223 \pm 243	431 \pm 30	3.8 \pm 0.2	0.05 \pm 0.01
B3: Annealed*	1151 \pm 17	304 \pm 6	0.27 \pm 0.01	0.34 \pm 0.02

*The annealing temperature of 773 K and annealing time of 3 hours

From the Table 2 and 3, the Seebeck coefficients of the non-annealed and annealed samples are in the range of 300-400 $\mu\text{V/K}$ and 200-300 $\mu\text{V/K}$, respectively. It can be seen that the thermoelectric power (S) of the Na-Co-O films are considerably improved, as compared to those of the pellet $\text{Na}_x\text{Co}_2\text{O}_4$ samples used as the sputtering target [35], which gave the Seebeck

Therefore, the annealed Na-Co-O films are not containing Co_3O_4 , at least as a majority phase. In other words, the annealed films are $\text{Na}_x\text{Co}_2\text{O}_4$, which possibly having Co_3O_4 as a second phase. The occurrence of Co_3O_4 is possible, just like that observed in the sintered pellet [35].

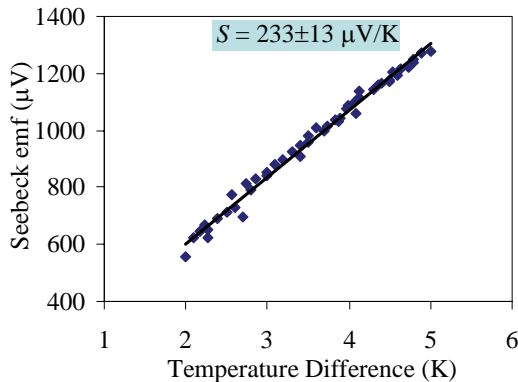


Fig. 7. Seebeck emf of the Na-Co-O film as a function of temperature difference. From this plot the Seebeck coefficient of $233 \pm 13 \mu\text{V/K}$ is obtained.

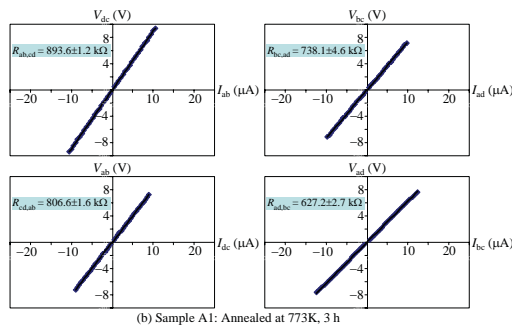


Fig. 8. Plot of the current-voltage characteristic for the measurement of resistivity. The resistivity obtained from these I - V plots is $0.42 \pm 0.01 \Omega \cdot \text{m}$.

The results shown in Table 2 and 3 indicate that samples of set B exhibits slightly better thermoelectric performance than samples of set A. For the non-annealed films, samples of set A gives the averaged Seebeck coefficients of $320 \mu\text{V/K}$ while that of the samples of set B is $422 \mu\text{V/K}$. Similar trend can be observed for the annealed films. Meanwhile, the electrical resistivity of the sample of set A is about 1.2 times as high as that of the sample B. These result in the power factor of sample of set B to be about twice as high as that of sample of set A. In addition to lower gas flow rate, i.e. lower gas pressure, the samples of set B were deposited at slightly higher sputtering power. This could promote the kinetic energy of the depositing species and lead to the denser film structure and the better thermoelectric performance. Another striking result in Table 2 and 3 is that although the post annealing of the as-deposited thin film results in the slight

decrease of the seebeck coefficient, the process leads to the decrease in the electrical resistivity of the films by an order of magnitude. This significantly improves the power factor by one order of magnitude after the post-annealing process. The results seem to correspond to the formation of the crystalline phase during the post annealing process, as observed in XRD measurement. It may be concluded that thermoelectric performance of the thin films can be improved with increasing discharge power and post-deposition annealing. However, the deposition of the thin films using the full range of deposition conditions must be further investigated to search for the optimum conditions for best thermoelectric performance.

4. Process Repeatability

Lastly, it is useful to point out the repeatability of the system. Table 2 and 3 present the thickness and the thermoelectric properties of Na-Co-O films deposited at the flow rate of 23.3 ± 0.1 sccm and 16.7 ± 0.1 sccm, respectively. At each flow rates, three sets of samples were prepared. It can be seen that at a given gas flow rate the discharge current and voltages can be repeated in an individual run and that there are small differences between the film properties of samples obtained from different runs. This indicates that good repeatability of the deposition process can be achieved from the built system. Therefore, it can be an important platform for further thin film research.

CONCLUSION

Pulsed-dc magnetron plasmas were successfully generated to enable the deposition of the Na-Co-O containing thin films from the $\text{Na}_x\text{Co}_2\text{O}_4$ ($x > 1.5$) target onto the glass substrates. The as-deposited films were amorphous. The films annealed at 773 K for 3 hours were possibly $\text{Na}_x\text{Co}_2\text{O}_4$ with Co_3O_4 phase as a second phase. All film samples exhibited p-type conduction. The as-deposited and annealed films showed the larger thermoelectric power, higher electrical resistivity, and, hence, lower power factor than the pellet used as the sputtering target. The thermoelectric properties of the Na-Co-O thin films are dependent on the discharge power during sputtering cycle and the gas flow rate. Namely, the thermoelectric power increased with increasing the discharge power and decreasing gas flow rate. In addition, it was found that the

annealing process at 773 K, in air, improved the power factor by one order magnitude. The preliminary studies in this work showed that repeatability of the deposition process and thin film properties can be achieved from the built system. Therefore, it can be used as an important platform for further thin film research.

ACKNOWLEDGMENT

This work was financially supported by the Commission on Higher Education (Ministry of Education), the Physics Department, Faculty of Science, Khon Kaen University and Loei Rajabhat University.

REFERENCES

- [1] L.M. Goncalves, C. Couto, P. Alpuim, D.M. Rowe and J.H. Correia, *Sens. Actua. A* 130 (2006) 346.
- [2] H. Wang, W.D. Porter, J. Sharp, International Conference on Thermoelectrics, Dallas, Texas: IEEE, (2005) 91.
- [3] M. Jansen and R. Hoppe, *Chem.* 408(2) (1974) 104.
- [4] I. Terasaki, Y. Sasago, K. Phys. Rev. B. 56(20) (1997) 12685.
- [5] T. Nagira, M. Ito, S. Katsuyama, K. Mjima and H. Nagai, *J. Alloys Comp.* 348 (2003) 263.
- [6] M. Ito, T. Nagira, D. Furumoto, S. Katsuyama and H. Nagai, *Scrip Mater.* 48(4) (2003) 403.
- [7] M. Ito, T. Nagira, D. Furumoto, Y. Oda and S. Hara, *Sci. Technol. Adv. Mater.* 5 (2004) 125.
- [8] T. Seetawan, V. Amornkitbamrung, T. Burinprakhon, S. Maensiri, K. Kurosaki, H. Muta, M. Uno, S. Yamanaka, *J. Alloy. Comp.* 403 (2005) 308.
- [9] T. Seetawan, V. Amornkitbamrung, T. Burinprakhon, S. Maensiri, K. Kurosaki, H. Muta, M. Uno, S. Yamanaka, *J. Alloy. Comp.* 407 (2006) 314.
- [10] T. Seetawan, V. Amornkitbamrung, T. Burinprakhon, S. Maensiri, K. Kurosaki, H. Muta, M. Uno, S. Yamanaka, *J. Alloy. Comp.* 414 (2006) 293.
- [11] T. Seetawan, V. Amornkitbamrung, T. Burinprakhon, S. Maensiri, P. Tongbi, K. Kurosaki, H. Muta, M. Uno, S. Yamanaka, *J. Alloy. Comp.* 416 (2006) 291.
- [12] R. Venkatasubramaniam, E. Siivola, T. Colpitts, B. O'Quinn, *Nature* 413 (2001) 597.
- [13] H. Suematsu, K. Kitajima, I. Ruiz, K. Kobayashi, M. Takeda, D. Shimbo, T. Suzuki, W. Jiang, *Thin Solid Films* 407 (2002) 132.
- [14] L.T. Zhang, M. Tsutsui, K. Ito, M. Yamaguchi, *Thin Solid Films* 443 (2003) 84-90.
- [15] J. Dheepa, R. Sathyamoorthy, S. Velumani, A. Subbarayan, K. Natarajan and P.J. Sebastian, *Sol. Energ. Mater. Sol. Cells.* 81 (2004) 305.
- [16] A.N. Banerjee, R. Maity, P.K. Ghosh, K.K. Chattopadhyay, *Thin Solid Films* 474 (2005) 261.
- [17] S.L. Huang, K.Q. Ruan, X.L. Jiao, H.Y. Wu, Z.M. Lv, Z.Q. Pang, J. Liu, H.S. Yang, W.B. Wu, L.Z. Cao and X.G. Li, *Phys. Lett. A.* 363 (5) (2007) 473.
- [18] J.Y. Son, Y.H. Shin and C.S. Park, *J. Solid State Chem.* 181 (2008) 2020.
- [19] X.P. Zhang, Y.S. Xiao, H. Zhou, B.T. Xie, C.X. Yang and Y.G. Zhao, *Mater. Sci. Forum.* 3807 (2005) 475.
- [20] H. Zhou, X.P. Zhang, B.Y. Xie, Y.S. Xiao, C.X. Yang, Y.J. He and Y.G. Zhao, *Thin Solid Films* 497 (2006) 338.
- [21] A. Venimadhav, Z. Ma, Q. Li, A. Soukiassian, X.X. Xi, D.G. Schlom, R. Arroyave, Z.K. Liu, M. Lee and N.P. Ong, *Mater. Res. Soc.* 886 (2006) 0886.
- [22] G.O. Este and W.D. Westwood, *Handbook of Thin Film Process Technology* 98(1) (1998).
- [23] W.J. Lee, Y.K. Fang, J.J. Ho, C.Y. Chen, S.F. Chen, R.Y. Tsai, D. Huang and F.C. Ho, *J. Electron. Mater.* 13 (2002) 751.
- [24] J. Wang, W. Lauwerens, E. Wieers, L.M. Stals, J. He and J.P. Celis, *Surf. Coat. Tech.* 153 (2002) 166.
- [25] J.L. Andújar, M. Vives, C. Corbella and E. Bertran, *Diamond Rel. Mater.* 12 (2003) 98.
- [26] J. Park, D.J. Kim, Y.K. Kim, Ke.H. Lee, Ki.H. Lee and H. Lee, *Thin Solid Films* 435 (2003) 102.
- [27] M. Åstrand, T.I. Selinder, F. Fietzke and H. Klostermann, *Surf. Coat. Tech.* 188 (2004) 186.
- [28] M. Fink, C. Löcker, J. Laimer, C. Mitterer and H. Störi, *Surf. Coat. Tech.* 188 (2004) 281.
- [29] H.C. Barshilia, B. Deepthi, A.S. Arun Prabhu and K.S. Rajam, *Surf. Coat. Tech.* 201 (2006) 329.
- [30] H.C. Barshilia and K.S. Rajam, *Surf. Coat. Tech.* 201 (2006) 1827.
- [31] J.M. Schneider, W.D. Sproul, *Handbook of Thin Film Process Technology* 98(1) (1998).
- [32] J. Sellers, *Surf. Coat. Tech.* 98(1) (1998) 1245.
- [33] W. Somkhunthot, T. Burinprakhon, I. Thomas, V. Amornkitbamrung, *T. Seetawan, ELEKTRIKA* 9(2) (2007) 20.
- [34] W. Somkhunthot, T. Burinprakhon, N. Pimpabute, I. Thomas, V. Amornkitbamrung, *KKU Res. J.*, 13(2) (2008) 168.
- [35] W. Somkhunthot, T. Burinprakhon, N. Pimpabute, T. Seetawan, A. Charoenphakdee, V. Amornkitbamrung, *Phys. Chem. Indian J.* 3(2-3) (2008) 347.
- [36] Yu. Ralchenko, A.E. Kramida, J. Reader, NIST ASD Team, NIST Atomic Spectra Database. (2008). Retrieved March 3, 2009, from http://physics.nist.gov/PhysRefData/ASD/lines_form.html.
- [37] Keithley Instruments, Inc., Low Level Measurements (28755 Aurora Road, Cleveland, Ohio 44139, U.S.A.); section entitled: "Van der Pauw Resistivity Measurements of Conductors". (1988). Retrieved March 16, 2009, from <http://www.keithley.com>.
- [38] L.D. Kadam and P.S. Patil, *Mater. Chem. Phys.* 68 (2001) 225.